Article | Received 24 September 2026; Revised 3 November 2026; Accepted 5 November 2026; Published 1X November 2026
https://doi.org/10.55092/aic20260016

Carrier frequency offset position detection in an OOK backscatter communication system for ambient internet of things

Xun Zhou[1], Yingchun Fu[2], Jinfeng Liang[3], Gongpu Wang[1] and Guochao Song[4,*]

[1] Beijing Jiaotong University, Beijing, China
[2] Zhongguancun Xinhaizeyou Technology Co., Ltd., Beijing, China
[3] Beijing Public Utility Science Research Institute Co., Ltd., Beijing, China
[4] China Academy of Information and Communications Technology, Beijing, China

* Correspondence author; E-mail: songguochao@caict.ac.cn.

Abstract: In this paper, we study the problem of carrier frequency offset (CFO) onset-position detection in an on-off keying (OOK) backscatter communication system, where the CFO may appear after an unknown transmission period. Different from conventional CFO estimation studies that mainly focus on estimating the frequency-offset value, this work aims to identify the first sample position at which the CFO occurs. To this end, the received complex-valued signal is transformed into a processed amplitude sequence through DC removal and a modulus operation, and the CFO onset detection problem is formulated as a change-point detection problem. We show that the statistical change caused by the CFO can be captured by a cumulative-sum (CUSUM)-based detector, while a bootstrap confidence test can be used to validate the detected change point. Simulations are then provided to evaluate the proposed method under different signal-to-noise ratios (SNRs), normalized CFO values, and CFO onset positions. The results show that the proposed CUSUM-based method provides stable CFO onset localization across the investigated conditions and generally demonstrates more consistent performance than the sliding-window and binary segmentation (BS) baselines.

Keywords: ambient internet of things; OOK backscatter communication; carrier frequency offset; onset-position detection; change-point detection; cumulative sum

1. Introduction

Ambient Internet of Things (Ambient IoT), also known as passive IoT, is emerging as a promising technology for large-scale, low-cost, and maintenance-free sensing networks. Unlike conventional IoT devices powered by batteries and active radio-frequency transmitters [1], Ambient IoT tags harvest energy from the surrounding environment and convey information through backscatter communication. Since the early demonstration of ambient backscatter communication [2], backscatter technology has been extended

Copyright©2026 by the authors. Published by ELSP. This work is licensed under Creative Commons Attribution 4.0 International License, which permits unrestricted use, distribution, and reproduction in any medium provided the original work is properly cited.

to commercial Wi-Fi [3], LoRa [4], and cellular networks [5]. Related studies have also investigated mobility-aware federated learning and service migration in vehicular edge computing networks [6,7]. Beyond these conventional connectivity scenarios, ambient backscatter has also been integrated with non-orthogonal multiple access (NOMA). Li *et al.* analyzed the effective capacity of ambient backscatter communication assisted non-orthogonal multiple access (AmBC-NOMA) communication systems under different quality-of-service constraints [8]. Li *et al.* further investigated physical-layer authentication for AmBC-aided NOMA symbiotic systems to enhance access security [9]. Recent studies have further summarized practical prototypes, major challenges, and future development directions of backscatter communication [10,11]. Meanwhile, 3GPP has investigated Ambient IoT support within the 5G-Advanced framework [12], and IEEE 802.11 has developed wake-up-radio mechanisms for ultra-low-power devices [13]. These advances indicate that Ambient IoT is progressing from academic feasibility studies toward standardization and practical deployment.

However, the low cost and extremely low power consumption of passive tags are accompanied by severe hardware limitations. Carrier frequency offset (CFO), caused by oscillator mismatch, environmental variation, or relative motion, is one of the major impairments affecting reliable backscatter reception. Conventional active transceivers generally employ stable clocks, sufficient power supplies, and strong signal-processing capabilities, allowing CFO to be estimated and compensated through synchronization algorithms. Recent studies on movable antenna systems have further shown that active wireless systems can improve communication and sensing performance through antenna-position optimization, precoding, and decoding design [14,15]. In contrast, passive tags cannot support high-quality oscillators, complex frequency-control circuits, or actively reconfigurable hardware. More importantly, in dynamic Ambient IoT environments, CFO may begin at an unknown time rather than remain present throughout the entire received sequence. Therefore, locating the position where CFO first appears is important for subsequent synchronization, estimation, and signal recovery.

CFO estimation has been widely studied in conventional wireless systems. Singh *et al.* reviewed blind CFO estimation techniques and compared their accuracy, complexity, and implementation requirements [16]. Pärlin *et al.* developed an adaptive filtering method for jointly tracking wireless channels, CFO, and sampling frequency offset [17]. Hussien *et al.* introduced gradient boosting machines for CFO estimation in 5G NR systems [18]. Although these methods improve frequency-offset estimation, they generally assume active transceivers with sufficient computational resources and predefined signal structures.

Several studies have therefore considered CFO under the specific channel and hardware characteristics of Ambient IoT and backscatter systems. Abdallah *et al.* proposed a semi-blind method for jointly estimating the channel, CFO, and I/Q imbalance [19]. Xu *et al.* investigated channel estimation and pilot design for Ambient IoT systems with frequency offsets, derived the corresponding performance bounds, and designed pilot sequences to reduce estimation error [20]. Hu *et al.* exploited frequency-domain sparsity and applied FML-AMP and NOMP algorithms to CFO estimation [21]. Singh *et al.* developed an attention- and SE-Net-based architecture for CFO estimation under multipath propagation and hardware impairments [22].

Nevertheless, existing studies mainly focus on estimating the CFO value, the channel, or multiple impairment parameters, usually assuming that CFO is already present over the observation interval. In contrast, identifying the first sample at which CFO appears is a distinct problem that has received comparatively

limited attention. This task is particularly challenging in on-off keying (OOK) backscatter systems because random switching between reflecting and non-reflecting states may obscure the statistical variation caused by CFO.

To address this issue, this paper investigates CFO onset-position detection in an OOK backscatter communication system by formulating it as a change-point detection problem. An OOK signal model with an unknown CFO onset position is first established. The received signal is then processed through direct current (DC) removal and a modulus operation to construct a real-valued detection sequence. A cumulative-sum (CUSUM) method is employed to estimate the CFO onset position, and a bootstrap confidence test is used to validate the detected change. Sliding-window mean-difference and basic binary segmentation detectors are included as baselines. The proposed method is evaluated under different signal-to-noise ratios(SNRs), CFO values, and CFO onset positions.

2. System model

Consider a typical backscatter communication system illustrated in Figure 1. The system consists of three entities: a signal source, a backscatter tag (device), and a reader (base station). The carrier wave (CW) source broadcasts a carrier wave signal to energize the tag. Then the tag modulates and backscatters the CW signal to the reader. Next the reader receives the superposition of the direct-link signal from the source and the backscattered signal from the tag.

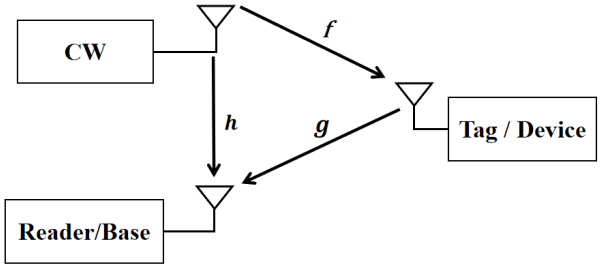


Figure 1. A backscatter communication system model.

The CW signal from the source $S_c(t)$ is

$$S_c(t) = \sqrt{P_c} \cdot e^{j(2\pi f_c t + \theta_c)}, \tag{1}$$

where P_c, f_c, θ_c denote the transmit power, carrier frequency, and initial phase of the source, respectively.

The signal propagates to the tag through the forward channel, denoted by the complex coefficient f. Thus, the received signal at the tag is:

$$x(t) = fS_c(t). \tag{2}$$

The tag transmits its information symbol $D(t)$ onto the incident carrier. This process alters the reflection coefficient of the tag antenna, resulting in the backscattered signal:

$$a(t) = \eta D(t) x(t), \tag{3}$$

where η represents the complex reflection efficiency.

The reader observes the signals from two paths: the direct path from the source with channel coefficient h, and the backscattered path from the tag with channel coefficient g. Additional additive white

Gaussian noise (AWGN) $\widetilde{w}(t)$ is also present. Therefore, the received passband signal at the reader is given by:

$$\widetilde{y}(t) = hS_c(t) + ga(t) + \widetilde{w}(t). \tag{4}$$

The reader down-converts the received signal $\widetilde{y}(t)$ using a local oscillator (LO) with frequency f_r and phase θ_r. The down-converted baseband signal is:

$$y(t) = \widetilde{y}(t)\, e^{-j(2\pi f_r t + \theta_r)}. \tag{5}$$

The difference between f_c and f_r from crystal oscillators is the CFO

$$\Delta f = f_r - f_c. \tag{6}$$

In Ambient IoT systems, the limited hardware and energy resources of passive tags constrain conventional CFO compensation, motivating the investigation of CFO-related signal characteristics at the reader.

Substituting Equations (1), (3), and (4) into Equation (5), and defining the phase offset $\Delta\theta = \theta_r - \theta_c$, we can have

$$\begin{aligned} y(t) &= [hS_c(t) + \eta g D(t) f S_c(t) + \widetilde{w}(t)] e^{-j(2\pi f_r t + \theta_r)} \\ &= [h + \eta g f D(t)] S_c(t) e^{-j(2\pi f_r t + \theta_r)} + n(t) \\ &= \sqrt{P_c} e^{-j(2\pi \Delta f t + \Delta\theta)} [h + \eta f g D(t)] + n(t) \end{aligned} \tag{7}$$

where

$$n(t) = \widetilde{n}(t)\, e^{-j(2\pi f_r t + \theta_r)} \tag{8}$$

is the baseband equivalent noise.

The continuous-time baseband signal is sampled with a period T_s. By substituting $t = nT_s$, where n denotes the discrete time index, we obtain the sampled signal:

$$\begin{aligned} y[n] &= y(t = nT_s) \\ &= \sqrt{P_c} e^{-j(2\pi \Delta f n T_s + \Delta\theta)} [h + \eta f g D[nT_s]] + n[nT_s] \end{aligned} \tag{9}$$

where $D[n] = D(nT_s)$ represents the discrete tag symbol and $\omega[n] = n(nT_s)$ is the discrete-time noise sample.

To simplify notation, we normalize the sampling period T_s to unity. Furthermore, we define the direct channel component as $h_0 = he^{-j\Delta\theta}$ and the composite backscatter channel as $h_1 = \eta f g e^{-j\Delta\theta}$. Consequently, the compact discrete-time model is expressed as:

$$y[n] = \sqrt{P_c} e^{-j2\pi \Delta f n} (h_0 + h_1 D[n]) + \omega[n] \tag{10}$$

This equation characterizes the received signal as a linear superposition of the direct and backscattered paths, parameterized by the composite channel gains h_0 and h_1.

3. OOK backscatter signal model with CFO onset

For OOK modulation, the tag symbol $D[n]$ is modeled as a binary sequence. Specifically, $D[n] = 1$ denotes that the tag is in the reflecting state, while $D[n] = 0$ denotes that the tag is in the non-reflecting state. Therefore, the information of the passive tag is embedded in the amplitude variation of the backscattered component through the switching of the reflection state.

In practical passive backscatter communication systems, the CFO may appear after a certain transmission period due to oscillator mismatch, environmental variation, or relative motion. In this study, we consider a single abrupt CFO onset, representing a transition from a frequency-aligned state to a state with a constant nonzero frequency offset. Let n_0 denote the unknown CFO onset position. The normalized CFO is modeled as

$$\Delta f[n] = \begin{cases} 0, & 1 \le n \le n_0, \\ \Delta f, & n_0 < n \le N. \end{cases} \tag{11}$$

Accordingly, the received signal in Equation (10) can be rewritten as

$$y[n] = \sqrt{P_c} e^{-j2\pi \Delta f[n] n} \left(h_0 + h_1 D[n]\right) + \omega[n]. \tag{12}$$

Before the CFO appears, the received signal is expressed as

$$y_0[n] = \sqrt{P_c} \left(h_0 + h_1 D[n]\right) + \omega[n], \quad 1 \le n \le n_0. \tag{13}$$

After the CFO appears, the received signal becomes

$$y_1[n] = \sqrt{P_c} e^{-j2\pi \Delta f n} \left(h_0 + h_1 D[n]\right) + \omega[n], \quad n_0 < n \le N. \tag{14}$$

More general scenarios involving gradual CFO variations or multiple change points are beyond the scope of the present single-onset model and will be considered in future work.

4. CUSUM-Based CFO onset detection

To detect the CFO onset position, we first transform the received complex-valued samples into a real-valued detection sequence. The sample mean of the received signal is calculated as

$$\bar{y} = \frac{1}{N} \sum_{n=1}^{N} y[n], \tag{15}$$

and the DC-removed residual signal is obtained by

$$r[n] = y[n] - \bar{y}. \tag{16}$$

Then, the modulus of the residual signal is used as the detection statistic:

$$z[n] = |r[n]|. \tag{17}$$

The DC removal suppresses the static component of the received signal, while the modulus operation converts the residual complex-valued signal into an amplitude sequence. When no CFO is present, the processed sequence $z[n]$ is mainly determined by the OOK-modulated backscatter component and noise. When CFO appears, the rotating phase term changes the residual component after DC removal, leading to a variation in the statistical characteristics of $z[n]$. To illustrate this effect, Figure 2 shows a representative realization of $z[n]$ before and after the CFO appears. The vertical red line indicates the actual CFO onset position. This observation provides an intuitive basis for formulating the CFO onset detection as a change-point detection problem.

The cumulative sum of the processed sequence is calculated as

$$S_k = \sum_{n=1}^{k} \left(z[n] - \bar{z}\right), \quad k = 1, 2, \ldots, N, \tag{18}$$

where

$$\bar{z} = \frac{1}{N}\sum_{n=1}^{N} z[n]. \tag{19}$$

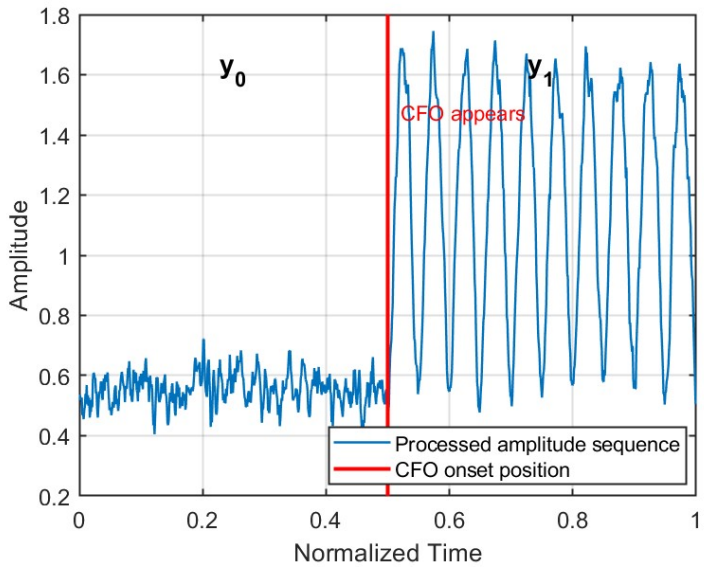


Figure 2. Processed signal feature before and after the CFO appears.

The CUSUM statistic accumulates the deviation of $z[n]$ from its global mean. If the statistical property of $z[n]$ changes after the CFO appears, the cumulative deviation will be amplified around the change point. Therefore, the CFO onset position is estimated as

$$\hat{n}_0 = \arg\max_{1\le k\le N} |S_k|. \tag{20}$$

To further determine whether a significant change exists, a bootstrap-based confidence test is employed. The processed sequence $z[n]$ is randomly permuted B times. For the b-th permuted sequence, the corresponding cumulative sum $S_k^{(b)}$ is calculated, and its maximum variation is defined as

$$S_{\text{diff}}^{(b)} = \max_{1\le k\le N} S_k^{(b)} - \min_{1\le k\le N} S_k^{(b)}. \tag{21}$$

For the original sequence, the maximum CUSUM variation is given by

$$S_{\text{diff}}^{(0)} = \max_{1\le k\le N} S_k - \min_{1\le k\le N} S_k. \tag{22}$$

The confidence level is calculated as

$$\text{CL} = \frac{1}{B}\sum_{b=1}^{B} \mathbb{I}\left(S_{\text{diff}}^{(b)} < S_{\text{diff}}^{(0)}\right) \times 100\%, \tag{23}$$

where $\mathbb{I}(\cdot)$ is the indicator function.

If CL exceeds 90%, the CFO is considered to exist. In this case, $\hat{n}_0$ is regarded as the detected position where the CFO first appears.

For comparison, a sliding-window mean-difference detector is also considered as a baseline method. This detector operates on the same processed sequence $z[n]$. For each candidate position k, two adjacent windows with length W are placed before and after k. The local mean values of the two windows are

calculated as

$$\bar{z}_k^- = \frac{1}{W} \sum_{n=k-W+1}^{k} z[n], \tag{24}$$

and

$$\bar{z}_k^+ = \frac{1}{W} \sum_{n=k+1}^{k+W} z[n]. \tag{25}$$

The corresponding mean-difference statistic is then given by

$$G[k] = \left| \bar{z}_k^+ - \bar{z}_k^- \right|. \tag{26}$$

The baseline detector estimates the CFO onset position as

$$\hat{n}_{\text{base}} = \arg \max_{W \le k \le N-W} G[k]. \tag{27}$$

This baseline provides a simple local mean-change detector and is used only for performance comparison with the proposed CUSUM method.

In addition, a basic binary segmentation (BS) detector is included as a second baseline. For each candidate position k, the processed sequence is divided into two segments, i.e., $z[1], \ldots, z[k-1]$ and $z[k], \ldots, z[N]$. The corresponding segment means are calculated as

$$\bar{z}_1(k) = \frac{1}{k-1} \sum_{n=1}^{k-1} z[n], \tag{28}$$

and

$$\bar{z}_2(k) = \frac{1}{N-k+1} \sum_{n=k}^{N} z[n]. \tag{29}$$

The BS statistic is defined as

$$G_{\text{BS}}(k) = \left| \bar{z}_1(k) - \bar{z}_2(k) \right|. \tag{30}$$

The estimated CFO onset position is then given by

$$\hat{n}_{\text{BS}} = \arg \max_k G_{\text{BS}}(k). \tag{31}$$

Since a single CFO onset is considered in the present signal model, only the first segmentation is used without further recursive partitioning.

5. Simulation results

To evaluate the proposed CFO onset detection method, numerical simulations are carried out based on the OOK backscatter signal model. Unless otherwise specified, the number of samples is set to $N = 1000$, the carrier power is set to $P_c = 1$, and the channel coefficients are set as $h_0 = 1.0e^{j\pi/6}$ and $h_1 = 0.4e^{j\pi/3}$.

To provide performance benchmarks, we included a sliding-window mean-difference detector with a window length of $W = 50$ and the basic BS detector for comparison. The proposed CUSUM method and the two baseline detectors operate on the same processed sequence and use identical OOK symbols and noise realizations. For each simulation point, 100 Monte Carlo trials are performed, and the average detected positions of the three methods are recorded. The number of bootstrap resamples is set to $B = 1000$, and the confidence-level threshold is set to 90%.

The sensitivity analysis shows that the detection probability remains unchanged when B varies from 200 to 2000 under the tested condition. Thus, $B = 1000$ is retained. The 90% confidence threshold provides a moderate balance between detection sensitivity and false-alarm control. For the sliding-window detector, a smaller window may achieve lower localization error under specific conditions. However, it can produce larger deviations over certain CFO ranges. Therefore, $W = 50$ is retained as a more balanced setting.

First, the effect of SNR on CFO onset detection is investigated. The normalized CFO is fixed at $\Delta f = 0.005$, and the CFO occurrence ratio is set to $t_1 : t_2 = 1 : 1$, corresponding to a theoretical CFO onset position of approximately 501. The SNR is varied from 0 to 30 dB.

As shown in Figure 3, the proposed CUSUM method maintains detected positions close to the theoretical position over the entire SNR range, demonstrating stable localization even at low SNRs. In contrast, the BS detector exhibits noticeable deviations at low SNRs before converging to the theoretical position, while the sliding-window detector shows larger deviations. These results demonstrate the stability of CUSUM under different SNR conditions.

Second, the influence of the CFO value is examined, as shown in Figure 4. With the other parameters unchanged, the CFO occurrence ratio is fixed at $t_1 : t_2 = 1 : 1$, and the theoretical CFO onset position is approximately 501. The normalized CFO is varied from 0.001 to 0.05 at an SNR of 10 dB. When the CFO is very small, the weak statistical change causes noticeable localization fluctuations. However, the proposed CUSUM method generally provides more accurate and stable results than the two baselines. The BS detector exhibits large deviations at several small CFO values, while the sliding-window detector shows fluctuations over a wider range. As the CFO increases, all three methods gradually converge to the theoretical position. These results highlight the advantage of CUSUM in localizing weak CFO variations.

Finally, the influence of the CFO onset position is evaluated, as shown in Figure 5. With the other parameters unchanged, the normalized CFO is fixed at $\Delta f = 0.005$, and the SNR is set to 15 dB. The theoretical CFO onset position is varied from approximately 100 to 900.

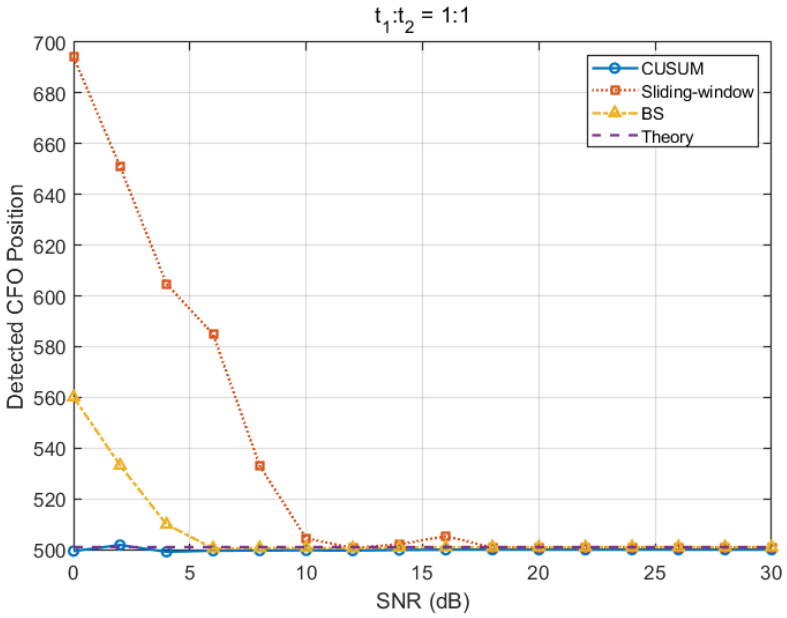


Figure 3. CFO position detection *versus* SNR for $t_1 : t_2 = 1 : 1$.

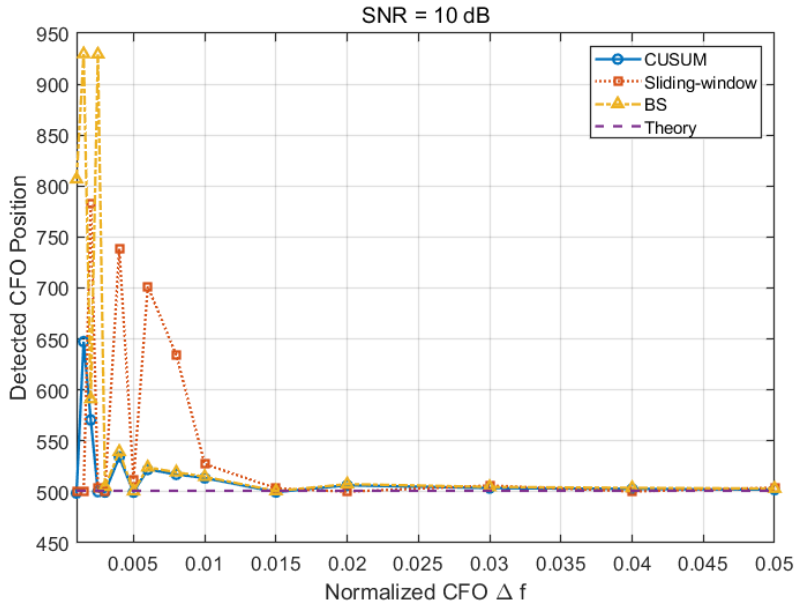


Figure 4. CFO position detection *versus* normalized CFO at an SNR of 10 dB.

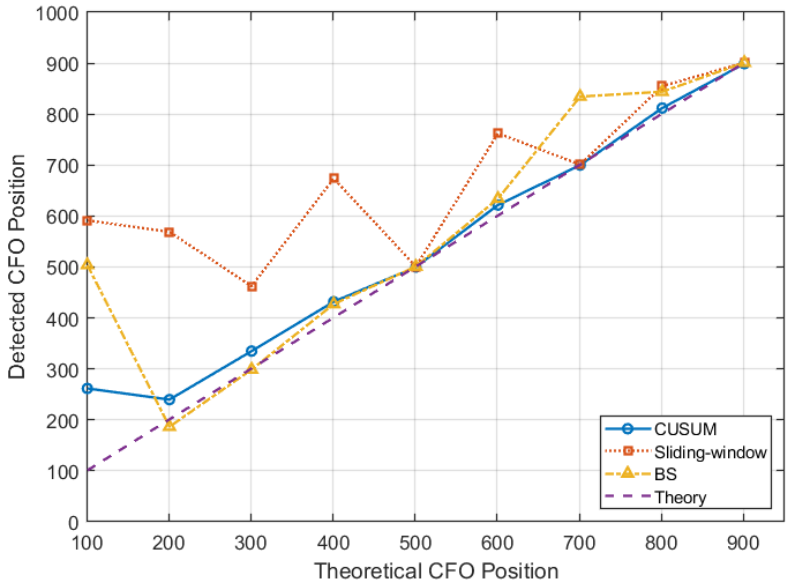


Figure 5. CFO position detection for different theoretical CFO onset positions.

The CUSUM results generally follow the theoretical onset positions, with larger deviations mainly near the beginning of the signal. In contrast, the BS detector exhibits noticeable deviations at several onset positions, including some later positions. This indicates that BS provides less consistent performance across different onset positions. The sliding-window detector shows even larger fluctuations, particularly at early and intermediate positions. Overall, CUSUM achieves more stable onset localization across the investigated range.

Overall, the simulation results demonstrate that the proposed CUSUM method can effectively localize the CFO onset under different SNRs, CFO values, and onset positions. Its performance generally improves as the SNR or CFO magnitude increases. Compared with the sliding-window and BS baselines, CUSUM provides more consistent localization across the investigated conditions, particularly for small CFO values.

The bootstrap confidence test further evaluates the reliability of CFO detection. With $P_D \geq 0.9$, the smallest tested normalized CFO values are 5×10^{-4}, 2×10^{-4}, 1×10^{-4}, and 1×10^{-4} at SNRs of 0, 5, 10, and 15 dB, respectively. The corresponding missed-detection probability is $P_{\text{miss}} = 1 - P_D \leq 0.1$. Under the no-CFO condition, the average false-alarm probability is $P_{\text{FA}} = 0.089$, close to the nominal level of 0.10. These results support reliable CFO detection under the considered conditions.

6. Conclusion

This paper investigated CFO onset-position detection in OOK backscatter communication systems. The received signal was transformed into an amplitude sequence, and a CUSUM-based method was employed to identify the unknown CFO onset position. A bootstrap confidence test was used to validate the detected change. Simulation results demonstrate effective and stable onset localization under different SNRs, CFO values, and onset positions. Compared with the sliding-window and BS baselines, the proposed method shows more consistent performance, particularly under small CFO conditions.

Data availability statement

The simulation data supporting the findings of this study are available from the corresponding author upon reasonable request.

Declaration of generative AI and AI-assisted technologies

During the preparation of this manuscript, the authors used ChatGPT to assist with language editing and improving readability. The authors reviewed and verified the manuscript and take full responsibility for its content.

Acknowledgments

This work was supported by the Deep Earth Probe and Mineral Resources Exploration–National Science and Technology Major Project (Grant No. 2025ZD1005200), the Beijing Natural Science Foundation (Grant No. L244008), and the National Natural Science Foundation of China (Grant No. U22B2004).

Authors' contribution

Conceptualization, G.S. and G.W.; methodology, X.Z. and G.S.; software, X.Z.; validation, G.S., Y.F. and J.L.; formal analysis, X.Z. and G.W.; investigation, X.Z., Y.F. and J.L.; resources, Y.F. and G.W.; data curation, X.Z. and J.L.; writing—original draft preparation, X.Z.; writing—review and editing, G.S., Y.F., G.W. and J.L.; visualization, X.Z. and J.L.; supervision, G.S. and G.W. All authors have read and agreed to the published version of the manuscript.

Conflicts of interest

Author Yingchun Fu and Author Jinfeng Liang are employees of Zhongguancun Xinhaizeyou Technology Co., Ltd. and Beijing Public Utility Science Research Institute Co., Ltd. The authors declare that this affiliation does not influence the design, analysis, interpretation, or presentation of the results reported in this manuscript.The authors declare no conflicts of interest.

References

[1] Qi Y, Li S, Zhou Y, Shi J. Communication-efficient participant selection for crowd-sensing in internet of vehicles with heterogeneous sensing, communication, and computing resources. *IEEE Internet Things J.* 2024, 12(1):1002–1015.

[2] Liu V, Parks A, Talla V, Gollakota S, Wetherall D, *et al.* Ambient backscatter: wireless communication out of thin air. In *Proceedings of the ACM SIGCOMM Conference*, Hongkong, China, August 12–16, 2013, pp. 39–50.

[3] Bharadia D, Joshi KR, Kotaru M, Katti S. BackFi: high throughput WiFi backscatter. In *Proceedings of the 2015 ACM Conference on Special Interest Group on Data Communication*, London, UK, August 17–21, 2015, pp. 283–296.

[4] Talla V, Hessar M, Kellogg B, Najafi A, Smith JR, *et al.* LoRa backscatter: enabling the vision of ubiquitous connectivity. *Proc. ACM Interact. Mobile Wearable Ubiquitous Technol.* 2017, 1(3):1–24.

[5] Feng Y, Chen S, Xi W, Wang S, Zhao J, *et al.* Heartbeating with LTE networks for ambient backscatter. *IEEE Trans. Mob. Comput.* 2024, 23(5):4246–4258.

[6] Peng Y, Tang X, Zhou Y, Hou Y, Li J, *et al.* How to tame mobility in federated learning over mobile networks? *IEEE Trans. Wireless Commun.* 2023, 22(12):9640–9657.

[7] Peng Y, Tang X, Zhou Y, Li J, Qi Y, *et al.* Computing and communication cost-aware service migration enabled by transfer reinforcement learning for dynamic vehicular edge computing networks. *IEEE Trans. Mob. Comput.* 2024, 23(1):257–269.

[8] Li X, Liu H, Li G, Liu Y, Zeng M, *et al.* Effective capacity analysis of AmBC-NOMA communication systems. *IEEE Trans. Veh. Technol.* 2022, 71(10):11257–11261.

[9] Li X, Wang Q, Zeng M, Liu Y, Dang S, *et al.* Physical-layer authentication for ambient backscatter-aided NOMA symbiotic systems. *IEEE Trans. Commun.* 2023, 71(4):2288–2303.

[10] Gu B, Li D, Ding H, Wang G, Tellambura C. Breaking the interference and fading gridlock in backscatter communications: state-of-the-art, design challenges, and future directions. *IEEE Commun. Surv. Tutorials.* 2025, 27(2):870–911.

[11] Cui Z, Wang G, Xu R, Wei X, Qin F, *et al.* Backscatter communications for green internet of things: practical prototypes, open challenges, and standardization. *IEEE Internet Things Mag.* 2025, 8(3):32–39.

[12] 3GPP. Study on solutions for Ambient IoT (Internet of Things) in NR. 2025. Available: https://portal.3gpp.org/desktopmodules/Specifications/SpecificationDetails.aspx?specificationId=4285 (accessed on 23 October 2026).

[13] IEEE. IEEE standard for information technology–telecommunications and information exchange between systems–local and metropolitan area networks-specific requirements–part 11: wireless LAN medium access control (MAC) and physical layer (PHY) specifications-amendment 3: wake-up radio operation. 2021. Available: https://standards.ieee.org/ieee/802.11ba/6896/ (accessed on 8 October 2021).

[14] Xiao Z, Li Z, Zhu L, Ning B, da Costa DB, *et al.* Movable antenna aided NOMA: joint antenna positioning, precoding, and decoding design. *IEEE Trans. Wireless Commun.* 2025, 25:4595–4612.

[15] Xiao Z, Pi X, Cao S, Zhu L, Gao Z, *et al.* Fundamental models and signal processing for movable antenna-enhanced wireless communications and sensing. *arXiv* 2025, arXiv:2511.05048.

[16] Singh S, Kumar S, Majhi S, Satija U, Yuen C. Blind carrier frequency offset estimation techniques for next-generation multicarrier communication systems: challenges, comparative analysis, and future prospects. *IEEE Commun. Surv. Tutorials* 2025, 27(1):1–36.

[17] Pärlin K, Riihonen T, Le Nir V, Adrat M. Estimating and tracking wireless channels under carrier and sampling frequency offsets. *IEEE Trans. Signal Process.* 2023, 71:1053–1066.

[18] Hussien M, Abdelmoaty A, Elsaadany M, Ahmed MFA, Gagnon G, *et al.* Carrier frequency offset estimation in 5G NR: introducing gradient boosting machines. *IEEE Access* 2023, 11:34128–34137.

[19] Abdallah S, Salameh AI, Saad M. Joint channel, carrier frequency offset and I/Q imbalance estimation in ambient backscatter communication systems. *IEEE Commun. Lett.* 2021, 25(7):2250–2254.

[20] Xu Y, Wang G, Xu R, Liu Y, Tellambura C, *et al.* Channel estimation and pilot design for ambient internet of things with frequency offsets. *IEEE Trans. Veh. Technol.* 2025, 74(3):5125–5129.

[21] Hu Q, Luo S, Liu M, Zhu J, Xu C, *et al.* Carrier frequency offset estimation in ambient internet of things. In *Proceedings of the 2025 IEEE 101st Vehicular Technology Conference (VTC2025-Spring)*, Oslo, Norway, June 17–20, 2025, pp. 1–5.

[22] Singh S, Singh SP, Majhi S, Satija U. A hybrid attention and SE-Net architecture for CFO estimation in MIMO-OFDM ambient backscatter communication systems. *IEEE Commun. Lett.* 2025, 30:377–381.